

Chair of Optoelectronics
Institute of Computer Engineering
Universität Heidelberg

Annual Report 2017

CONTENTS

Staff	II
Foreword	III
Research Projects	IV
Publications 2017	7
Imprint.....	8

STAFF



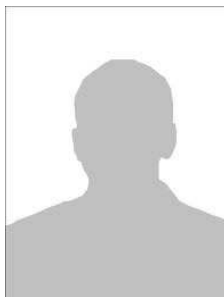
**Prof. Dr.
Karl-Heinz Brenner**
Head of the Chair



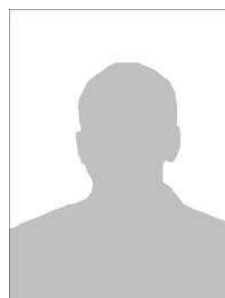
Sabine Volk
Secretary



Wolfgang Stumpfs
Technical Assistant



Rico Erhard
MSc-Student
(no picture available)



Sebastian Einsiedler
BSc-Student
(no picture available)



André Junker
PhD-Student



FOREWORD

Dear reader,

This is the last annual report issued by this research group. With the end of the Wintersemester 2017/2018, I will retire and the present chair of optoelectronics will reoriented to a new direction. After my retirement, I would be happy to find other challenging tasks in the field of optics.

This annual report describes the research activities for the years 2016-2017.

The contribution on page 1 describes an alternative method for phase reconstruction using the transport of intensity. Unlike previous approaches, here we use the three-dimensional version of the Helmholtz equation. The contribution on page 2 picks up on an old problem, the calculation of light propagation in strongly inhomogeneous media. The WPM method invented in 1992, although very accurate, was too slow for three-dimensional problems. With this approach, we achieved a speed-up in the order of 10^5 . The contribution on page 3 received a considerable amount of attention on the previous Diffractive optics meeting in Finnland. The subsequent publication in J. Opt. Soc. Am. received an even better response from the reviewers. It represents an alternative way of solving the RCWA-problem. By avoiding the eigenvalue decomposition, we now are able to solve really large problems. The previous approach for this problem size resulted in matrix sizes of several tens of TB and in compute times of years, whereas this approach requires moderate matrix sizes and finishes in minutes. The contribution on page 4 illustrates the steps necessary for RCWA modeling of 4π illumination microscopy and on page 5 we analyse the equivalence of spatial transformations and material parameters and with the last contribution we try to solve the incoherent imaging problem in light field microscopy.

We hope that many of the topics in this report will find your interest.

Karl-Heinz Brenner
Head of the chair

RESEARCH PROJECTS

Improved phase reconstruction by iterative solution of the three-dimensional Transport of Intensity equation <i>J. Postels, K.-H. Brenner</i>	1
A fast version of the wave propagation method applied to micro-optics <i>K.-H. Brenner</i>	2
Achieving a high mode count in the exact electromagnetic simulation of diffractive optical elements <i>A. Junker, K.-H. Brenner</i>	3
Bidirectional illumination in rigorous coupled-wave analysis <i>A. Junker, K.-H. Brenner</i>	4
Transformed diffraction gratings <i>R. Erhard, K.-H. Brenner</i>	5
Reconstruction of light field photography by deconvolution <i>S. Einsiedler, K.-H. Brenner</i>	6

Improved phase reconstruction by iterative solution of the three-dimensional Transport of Intensity equation

J. Postels, K.-H. Brenner

In the optical regime, light detectors are restricted to measuring the intensity of a light distribution. If phase is also of interest, one can apply either interferometric or noninterferometric methods. For the first method, coherent light from a laser and a reference wave is needed. Due to speckle problems associated with coherent methods, also noninterferometric methods are attractive. Typically these methods do not determine phase directly but rather the gradient of the phase. The methods based on the transport of intensity (TIE) have recently gained interest. The underlying principle is to deduce phase information from the change of intensity along propagation. The fundamental equation for intensity transport is derived from the imaginary part of the Helmholtz equation and is given by [1].

$$(\bar{\nabla}I)(\bar{\nabla}\phi) + I(\nabla^2\phi) = 0 \quad (1)$$

Typically this equation is used in its paraxial two dimensional form, initiated by Teague[2] and used by many successors, which reads

$$k \frac{\partial I}{\partial z} = -\nabla_{\perp} (I \nabla_{\perp} \phi) \quad (2)$$

We intentionally add the perpendicular suffix to emphasise that only the x- and y- derivatives are involved in this definition. For this work, we used the nonparaxial 3D version [3] given in eq. (1) but we assume that the phase can be split into a slow and a rapidly varying part

$$\phi(x, y, z) = kz + \varphi(x, y, z). \quad (3)$$

Then, the iteration is described by

$$\bar{\nabla}\phi_n(\bar{x}) = \mathfrak{S}_3^{-1} \left(\frac{i}{2\pi(v^2 + \mu^2 + \eta^2)} \begin{pmatrix} v \\ \mu \\ \eta \end{pmatrix} \cdot \mathfrak{S}_3 \left(\left(\frac{\bar{\nabla}I(\bar{x}) \cdot \bar{\nabla}\phi_{n-1}(\bar{x})}{I} \right) \right) \right) \quad (4)$$

where \mathfrak{S}_3 is the three dimensional Fourier operator and $\bar{\nabla}$ is the usual 3D-Gradient. v, μ and η are the spatial frequencies in the x-,y- and z-directions. The iteration operates only on the gradient of the phase and starts with $\bar{\nabla}\phi_0(\bar{x}) = (0, 0, k)$. Thus no numerical phase derivative has to be calculated. As a test phase object, we used a summation of four Gaussians shifted to different positions with different widths and heights. The maximum height was 16π . Thus the maximum phase gradient corresponds to a numerical aperture of 0.29, proving that the phase distribution is non-paraxial. Figures. 1 and 2 show the reconstructed phase difference and amplitude difference. Its maximum deviation of 0.001 rad corresponds to 1/6000 of a wave

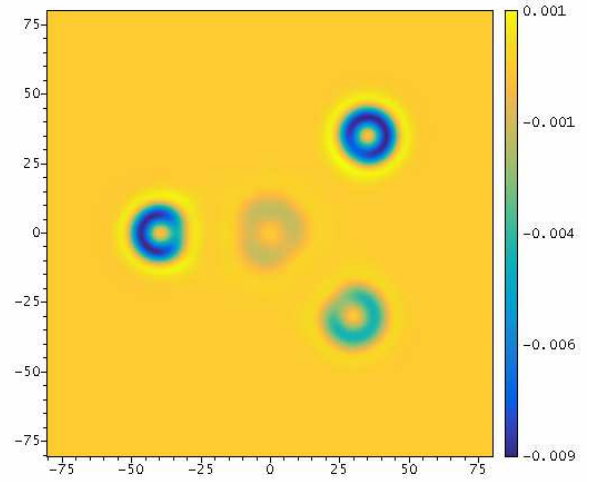


Fig. 1: Phase difference between original and reconstructed phase. Positions in μm .

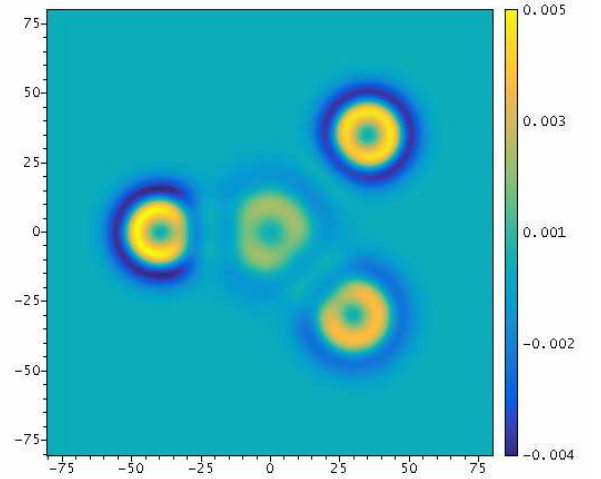


Fig. 2: Amplitude difference between original ($=1$) and reconstructed amplitude. Positions in μm .

and the amplitude deviation must be compared to the initial 1-amplitude. A crucial point is the spatial sampling, which has to be matched to the NA. The three dimensional TIE thus has to be considered as a very accurate method of phase reconstruction.

References:

- [1] M.A. Alonso, "Rays and waves", in Phase Space Optics: Fundamentals and Applications, (McGraw-Hill, 2009), eds. B. Hennelly, J. Ojeda-Castaneda, and M. Testorf
- [2] M.R. Teague, "Deterministic phase retrieval: a Green's function solution", J. Opt. Soc. Am. 73, No. 11, 1434-1441, (1983)
- [3] K.-H. Brenner, J. Postels, "Improved phase reconstruction by iterative Solution of the Transport of Intensity Equation", Jahrestagung der Deutschen Gesellschaft für angewandte Optik e. V., 17.-21. Mai 2016, Hannover, (2016)

A fast version of the wave propagation method applied to micro-optics

K.-H. Brenner

The wave propagation method (WPM) is a method that can accurately simulate inhomogeneous media at high numerical apertures in the micro-optical size range. Basically all optical systems, which are not adequately described by the thin element approximation must be considered as inhomogeneous media. For these types of media, a wide range of simulation methods is only available in the macroscopic and in the nanoscopic regime. In the macroscopic regime, ray tracing techniques are sufficiently accurate. In the nanoscopic regime, rigorous solutions of the Maxwell equations can be applied. For the in between regime of micro optics, neither of these methods is applicable. Ray tracing is insufficient due to its lack of treating diffraction. Rigorous solutions are not viable due to the large memory demand required. As an example, for a moderate micro-optical problem in the size of $(250\mu\text{m})^3$ an unreasonable size of 15 TB of core memory would be required for a RCWA calculation.

One of the few methods for treating nonparaxial propagation in inhomogeneous media is the wave propagation method [1,2]. Recently, the large computing time for 3D-problems could be reduced significantly [3,4,5], thus enabling rapid simulation for micro optical systems. Like the BPM, this method slices the volume into a finite number of thin layers with an index of refraction, which varies inside one layer only in the lateral x - and y -direction. But unlike the BPM, this method is not restricted to the paraxial domain and was demonstrated to be accurate for angles up to 85° [1]. Similar to the angular spectrum, the WPM is described by multiplication with a propagation kernel in the spectral domain. But unlike the angular spectrum, this kernel P is four-dimensional, since it also depends on the position coordinates.

$$u(\mathbf{r}_\perp, z + \delta z) = \iint \tilde{u}(\mathbf{v}_\perp, z) \times P(\mathbf{v}_\perp, \mathbf{r}_\perp) \exp(2\pi i \mathbf{v}_\perp \mathbf{r}_\perp) d^2 v_\perp \quad (1)$$

In the most general case, the computation thus is very time demanding and grows with the fourth power of the linear dimension. Recently, it was discovered [3,4,5] that the WPM can be accelerated significantly, if the number of different refractive indices appearing in the problem is small. We call this variant the Discrete Index WPM. In this case, the WPM algorithm in eq. (1) can be rewritten as a sum of angular spectrum calculations, which due to the availability of the fast Fourier transform can be performed in logarithmic time instead of polynomial time. For the typical problem size of $(250\mu\text{m})^3$, mentioned above with appropriate sampling, this corresponds to a speedup of 40000.

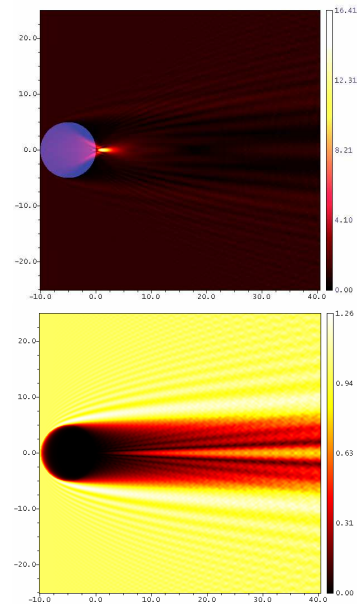


Fig. 1: Diffraction of light by a three-dimensional refracting $n = 1.5$ (top) and absorbing $n = 1+0.2i$ (bottom) sphere, matched to the index outside.

As one of many examples, in fig. 1 we considered the diffraction of light by a 3D-sphere with a diameter of $10 \mu\text{m}$. The top figure shows a refractive sphere with $n=1.5$. At the bottom, the refractive index of the sphere as well as the index outside are 1 and only absorption inside the sphere ($\kappa=0.2$) causes the diffracted waves. In conclusion, the discrete index version of the WPM has become fast enough for a rapid analysis of complex three-dimensional micro-optical systems with extremely high numerical apertures and sizes in the millimeter range.

References:

- [1] K.-H. Brenner, W. Singer, "Light propagation through micro lenses: a new simulation method", *Appl. Opt.*, Vol. 32, No. 26, pp. 4984-4988, (1993)
- [2] M. Fertig, K.-H. Brenner, "The vector wave propagation method (VWPM)", *J. Opt. Soc. Am. A*, Vol. 27, No. 4, pp. 709-717, (2010)
- [3] N. Lindlein, University of Erlangen, private communication, Jan. 2016
- [4] S. Schmidt, T. Tiess, S. Schröter, R. Hambach, M. Jäger, H. Bartelt, A. Tünnermann, and H. Gross, "Wave-optical modeling beyond the thin-element-approximation", *Optics Express.*, Vol. 24, No. 26, pp. 30188-30200, (2016)
- [5] K.-H. Brenner, "A high-speed version of the wave propagation method applied to micro-optics", 16th Workshop on Information Optics (WIO), IEEE Xplore Digital Library, Interlaken, Schweiz, (2017)

Achieving a high mode count in the exact electromagnetic simulation of diffractive optical elements

A. Junker, K.-H. Brenner

The application of rigorous optical simulation algorithms, both in the modal as well as in the time domain, is known to be limited to the nanooptical scale due to severe computing time and memory constraints. This is true even for today's high performance computers. In order to simulate the light propagation through a structured medium with an adequate sampling of, for instance, 1000^2 pixels, the rigorous coupled-wave analysis (RCWA) [1] already requires ~ 60000 years and ~ 4000 TB of RAM. To address this problem, the Fast Rigorous Iterative Method (FRIM) is presented, an algorithm based on an iterative approach, which, under certain conditions, allows solving also large size problems approximation free [2]. The principle relies on the basic equation used in RCWA,

$$\begin{pmatrix} \mathbf{S}_I \\ \mathbf{R} \end{pmatrix} = \hat{\Gamma} \begin{pmatrix} \mathbf{T} \\ \mathbf{S}_{II} \end{pmatrix}, \quad (1)$$

where \mathbf{S}_{III} , \mathbf{R} and \mathbf{T} are the incident, reflected and transmitted mode coefficients. As shown in [2], it is possible to implement a time and memory efficient scheme to multiply both $\hat{\Gamma}$ and $\hat{\Gamma}^{-1}$ to an arbitrary vector. The computationally complex eigenmode decomposition is completely avoided. Thereby, the numerical cost is reduced from $O(N^3)$ to $O(N \log N)$, bringing computing time and RAM size in a realistic

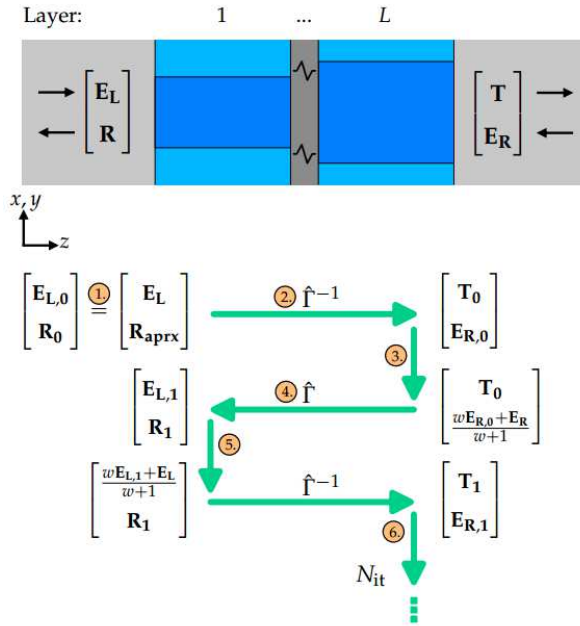


Fig. 1: FRIM iteration scheme: alternately apply $\hat{\Gamma}$ and $\hat{\Gamma}^{-1}$ to propagate the mode coefficients across the grating while partially mixing in the true incident light coefficients at each side given some mixing parameter $w \in \mathbb{R}^+$.

dimension. Fig. 1 shows the iterative scheme of the ‘fast rigorous iterative method’ (FRIM), which is based on eq. (1). As shown in [2], the convergence behavior of this procedure is exponential in the number of iterations. Convergence is generally reached if the grating is chosen sufficiently thin (up to a few wavelengths), if the numerical aperture of the calculation is less than one, and if the absorption of the medium is not too large. These conditions are ideal for the simulation of structures like, for instance, certain diffractive optical elements. With the FRIM, these can now be simulated with a significantly higher mode count than before. Apart from speed, another major advantage of the iterative FRIM over standard modal methods is the possibility to trade runtime against accuracy.

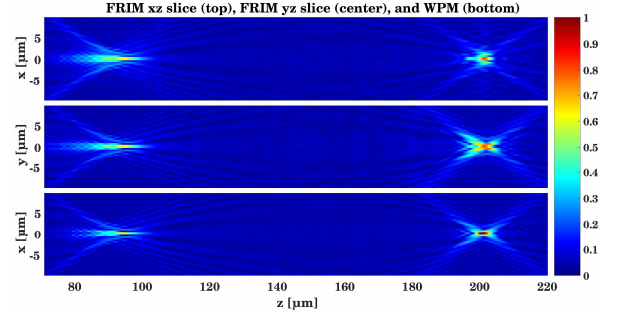


Fig. 2: Electric field amplitude behind a 2π -FZP for plane wave light incidence. Rigorous FRIM (top x-z slice; center y-z slice) and WPM (bottom x-z slice). $MO_{x/y} = 391$, $P_{x/y} = 300\mu\text{m}$, $\lambda = 532\text{nm}$, $NA_{\text{calc}} = 0.98$, $N_{\text{it}} = 18$.

Fig. 2 shows a sample simulation of a Fresnel zone plate (FZP) with phase jump 2π using the FRIM and the wave propagation method (WPM) [3] for comparison. Both simulations exhibit similar features and differ significantly from the form of a plane wave (the result of the thin element approximation). Differences between FRIM and WPM are observed in the focus form and amplitude. The latter are due to polarization effects, since the central x-z and y-z slices of the FRIM simulation feature significant differences.

References:

- [1] M. G. Moharam, T. K. Gaylord, E. B. Grann, and D. A. Pommet, ‘‘Formulation for stable and efficient implementation of the rigorous coupled-wave analysis of binary gratings’’, *J. Opt. Soc. Am. A* 12, 1068–1076, (1995)
- [2] A. Junker, K.-H. Brenner, ‘‘Achieving a high mode count in the exact electromagnetic simulation of diffractive optical elements’’, *J. Opt. Soc. Am. A*, Vol. 35, No. 3, 377–385, (2018)
- [3] K.-H. Brenner and W. Singer, ‘‘Light propagation through microlenses: a new simulation method’’, *Appl. Opt.* 32, 4984–4988, (1993)

Bidirectional illumination in rigorous coupled-wave analysis

A. Junker, K.-H. Brenner

The rigorous coupled-wave analysis (RCWA) is applied to the simulation of 4π -microscopy. To this end, the concept of structured illumination [1] is combined with the idea of coherent two-sided light incidence. It is shown how the latter can be integrated into the framework of the RCWA. These techniques are applied to simulate two coherent counter-propagating converging beams incident upon a sample as in 4π -microscopy. Consider Fig. 1, which shows the standard RCWA configuration with homogeneous incident / transmitted regions and a structured layer stack in the middle.

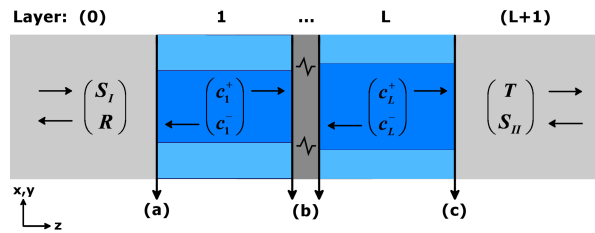


Fig. 1: Standard RCWA setup, bidirectional light incidence

In contrast to the standard RCWA, light incidence is also assumed from the right side, i.e. $S_{II} \neq 0$. In order to enforce the boundary conditions, either the S-matrix approach [2] or a modified ETMA [3] can be applied. In the S-matrix approach, the forward and backward propagating Fourier modes in the incident and transmitted region are connected via

$$\begin{pmatrix} \mathbf{R} \\ \mathbf{T} \end{pmatrix} = \begin{pmatrix} S_{11}^{\text{global}} & S_{12}^{\text{global}} \\ S_{21}^{\text{global}} & S_{22}^{\text{global}} \end{pmatrix} \begin{pmatrix} \mathbf{S}_I \\ \mathbf{S}_{II} \end{pmatrix}, \quad (1)$$

i.e. mathematically the only change is the replacement of a zero-vector by the non-zero vector \mathbf{S}_{II} . In the modified ETMA, some additional quantities need to be introduced as described in [3], but the general principle remains the same. In the two methods, both the numerical complexity and the required memory space to obtain the solution are not changed. In the following, the microscopic sample shown in Fig. 2 is illuminated with two coherent overlapping focused light beams (4π illumination), where the region prepared with the fluorescence markers is positioned at the center of the undisturbed 4π -focus. An x - z -slice through the aberrated 4π -focus is shown in Fig. 3 (bottom) in comparison to the unperturbed focus (top). It is observed that the aberrations introduced by the sample significantly change the form of the focus. The amplitude of the central peak is decreased and intensity is spilled into the side lobes, which are no longer arranged symmetrically around the central focus. In addition, the focus position is shifted in the z -direction by more than 100 nm out of its original central position.

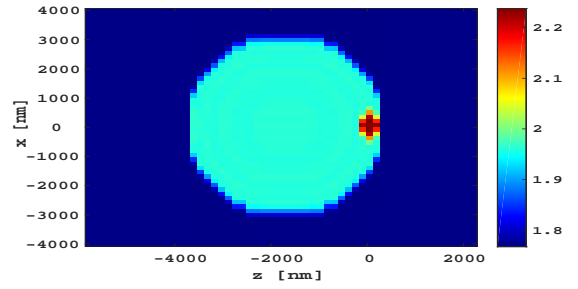


Fig. 2: Spatial permittivity distribution of the microscopic sample: ovoid protein envelope with diameters $4\mu\text{m} \times 6\mu\text{m} \times 4\mu\text{m}$ and $\epsilon = 1.96$ suspended in water ($n = 1.33$), containing another ovoid absorbing structure with diameters $0.8\mu\text{m} \times 0.8\mu\text{m} \times 0.4\mu\text{m}$ and $\epsilon = 2.24 + 0.3i$, which is prepared with fluorescence markers.

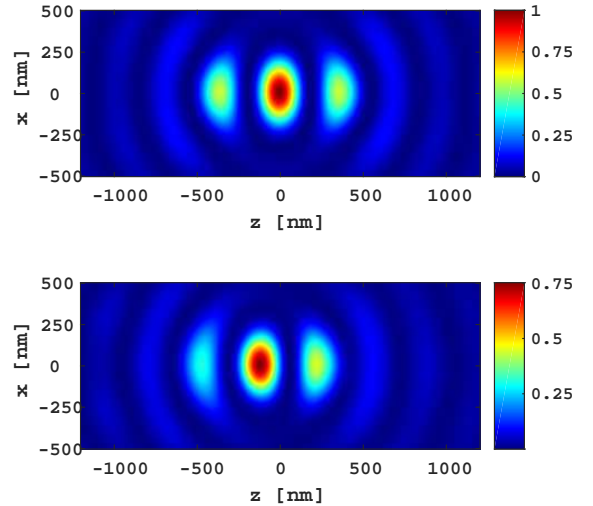


Fig. 3: Focus form of the unperturbed (top) vs. aberrated (bottom) 4π -focus. $MO_{x/y} = 20$, $P_{x/y} = 10\mu\text{m}$, $\lambda = 800\text{nm}$

With the combination of the above concepts, aberrations in microscopic systems, where polarization effects play a major role, can now be consistently simulated and therefore be better understood and avoided.

References:

- [1] M. Auer and K.-H. Brenner, "Localized input fields in rigorous coupled-wave analysis", J. Opt. Am. A 31, 2385-2393, (2014)
- [2] R. C. Rumpf, "Improved formulation of scattering matrices for semi-analytical methods that is consistent with convention", Prog. Electromagn. Res. B35, 241-261, (2011)
- [3] A. Junker, K.-H. Brenner, "Two-sided illumination in rigorous coupled-wave analysis applied to the 4π -microscope", J. Opt. Soc. Am. A 34, 1769-1775, (2017)

Transformed diffraction gratings

R. Erhard, K.-H. Brenner

Transformation optics is a theory based on the formal invariance of Maxwell's equations under coordinate transformations [1]. This formal invariance allows to relate transformations with changes in material parameters and with transformed electromagnetic fields. This relation can be exploited to design media that transform the electromagnetic fields according to the transformation used in the design. Having chosen a transformation, the material specification of the transformation medium is described by [2]

$$\tilde{\epsilon} = \frac{\Lambda \epsilon \Lambda^T}{|\Lambda|}, \quad \tilde{\mu} = \frac{\Lambda \mu \Lambda^T}{|\Lambda|} \quad (1)$$

where Λ is the Jacobian matrix of the transformation and ϵ is the electric permittivity and μ the magnetic permeability of the original medium.

We checked this formal invariance numerically by means of rigorous simulations of transformed diffraction gratings. The transformed gratings were designed with the recipe (1), applying transformations to ordinary diffraction gratings. The transformations were chosen to be continuous everywhere and to leave the region around the gratings untouched or only shifted with respect to the optical axis. In doing so, the transformed devices are expected to have the very same diffractive effects as their original counterparts apart from constant phase shifts.

The relative permittivity distribution of a 1D trapezoidal grating serving as a test sample is depicted in Fig. 1 (a). The transformation leading to the transformed grating is a polynomial

$$t(x) = a_1(z)x + a_3(z)x^3, \quad (2)$$

that maps the lateral contours of the original grating to the constant $x_a \approx \pm 1.074 \mu\text{m}$. On the left side of the grating domain the transformation is the identity. On the right side it is necessary to extend the transformation beyond the original grating domain to let it continuously approach the identity. The resulting transformed grating is anisotropic and inhomogeneous. Only the xx-component of its relative permittivity tensor is shown in Fig. 1 (b).

The diffraction efficiencies for both gratings were calculated with the S-matrix algorithm for perpendicular incident TE-polarised light of wavelength $0.633 \mu\text{m}$. The diffraction efficiencies with respect to the truncation level used in the differential method [3] are depicted in Fig. 2. They agree for large

enough truncation level as predicted by the theory albeit with small deviations. We attribute these deviations to numerical errors. Since the convergence of the far-field efficiencies for the transformed grating is comparable to that of the initial grating, this aspect does not provide a practical benefit, at least not in this example. For near field quantities, this aspect still needs to be investigated.

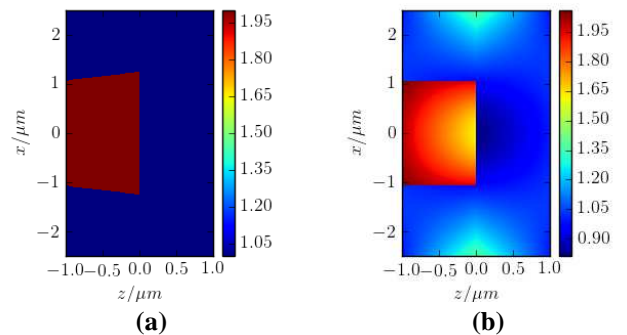


Fig 1: Relative permittivity distribution of the original grating (left) and the xx-component of the relative permittivity tensor of the transformed grating (right).

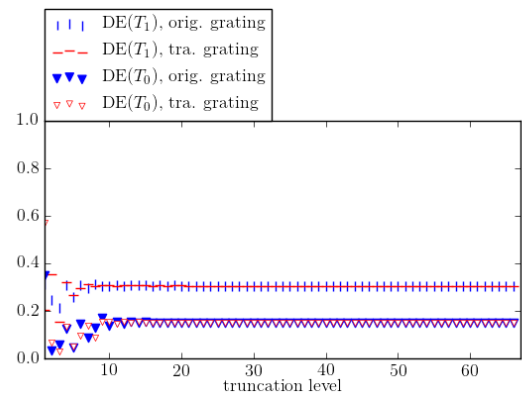


Fig 2: Comparison of the diffraction efficiencies of the transformed and the original grating with respect to the truncation level used in the differential method [3].

References:

- [1] J. Plebanski, Pys. Rev., 118.5, pp. 1396-1408, (1959)
- [2] D. Schurig, J. B. Pendry, D. R. Smith, Optics Express, Vol. 18, No. 21, pp. 9794-9804, (2006)
- [3] K. Watanabe, R. Petit, M. Nevière, J. Opt. Soc. Am. A, 19.2, pp. 325-33, (2002)

Reconstruction of light field photography by deconvolution

S. Einsiedler, K.-H. Brenner

A light field camera allows to acquire three-dimensional information of the photographed object. This additional information can be used to calculate refocused images in a different, selectable focal plane. The combination of several of these two-dimensional images can later be used to create an image with extended depth of field. The goal of this work is to use a wave optical deconvolution algorithm to calculate these images. A ray based technique was already successfully used for reconstruction [1].

Our plenoptic camera consists of a main lens, a micro lens array and a CCD-sensor. The object is projected onto the micro lens array before it hits the sensor. As a result, a huge number of micro images of the object appear on the sensor, all taken from slightly different angles. These micro images contain the three-dimensional information [1].

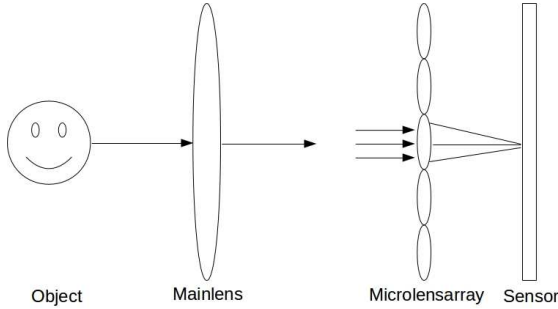


Fig. 1: Schematic setup of a light field camera

We consider the transformation from the object to the sensor as a linear and incoherent, but space variant operation H . The total imaging process is thus described by:

$$I(x_o, y_o) = \int |u(x_i, y_i)|^2 \cdot H(x_i, y_i, x_o, y_o) dx_i dy_i \quad (1)$$

$I(x_o, y_o)$ is the intensity distribution on the CCD-sensor. The subscript “ o ” denotes output coordinates and “ i ” denotes input coordinates.

The operator H can be determined by measuring the impulse response for every point (x_i, y_i) in the object.

Following Ref. [2] we discretize the object and the image, and obtain a linear algebraic equation:

$$I_{x_o, y_o} = \sum_{x_i} \sum_{y_i} |u_{x_i, y_i}|^2 H_{x_i, y_i, x_o, y_o} \quad (2)$$

The intensity vector I is the measured sensor intensity with the object as input and H is a matrix assumed as known. The mathematical problem, to be solved is thus the inversion of eq. (2).

The transformations from images into vectors and from a set of images M into a matrix is given by:

$$\vec{V}_{mN+n} = V_{m,n} \quad (3a)$$

$$M_{mN+n, m'N+n'} = H_{m, m', n, n'} \quad (3b)$$

Thus we can write shortly:

$$\vec{I} = H \cdot \vec{U} \quad (4)$$

Now $\vec{U} = |u|^2$ can be reconstructed in principle by solving this system of linear equations. We assume that H will be far too large to be kept in memory, even if we are able to find redundant information in H , caused by the periodic nature of the micro lens array. Therefore we will apply an iterative algorithm to invert eq. (4). Since we are in the middle of this project, we cannot show results now. But a complexity analysis predicts, that the wave optical method might be faster than the ray optical approach.

References:

- [1] Ren Ng “Digital light field photography”, Doctoral Dissertation, Stanford University, from cdn.lytro.com/renng-thesis.pdf, (2006)
- [2] Michael Broxton, Logan Grosenick, Samuel Yang, Noy Cohen, Aaron Andalman, Karl Deisseroth, and Marc Levoy, “Wave optics theory and 3-D deconvolution for the light field microscope”, *Opt. Express* **21**, 25418-25439, (2013)

PUBLICATIONS

1. K.-H. Brenner, S. Mehrabkhani, „Modification of Spatial Domain Algorithms for Apertureless Light Propagation“, Applied Optics 56, No. 1, A8 – A12, Doc.ID 273329, (2017)
2. A. Junker, K.-H. Brenner, “Two-sided illumination in rigorous coupled-wave analysis applied to the 4π -microscope”, J. Opt. Soc. Am. A, Vol. 34, No. 10, pp. 1769-1775, (2017)
3. INVITED: K.-H. Brenner, “A high-speed version of the wave propagation method applied to micro-optics”, 16th Workshop on Information Optics (WIO), IEEE Xplore Digital Library, 03.-07- Juli 2017, Interlaken, Schweiz, (2017)
4. A. Junker, K.-H. Brenner, „Bidirectional light incidence in rigorous coupled-wave analysis applied to 4π -microscopy“,16th Workshop on Information Optics (WIO), IEEE Xplore Digital Library, 03.-07- Juli 2017, Interlaken, Schweiz, (2017)
5. A. Junker, K.-H. Brenner, „High mode count rigorous simulation of diffractive optical elements by an iterative solution approach“, EOS Topical Meeting on Diffractive Optics (DO), ISBN 978-952-68553-4-9, 04.-07-September 2017, Joensuu, Finland, (2017)
6. A. Junker, K.-H. Brenner, “Achieving a high mode count in the exact electromagnetic simulation of diffractive optical elements”, J. Opt. Soc. Am. A, Vol. 35, No. 3, 377-385, (2018)

IMPRINT

Publisher: Prof. Dr. Karl-Heinz Brenner
Chair of Optoelectronics
Institute of Computer Engineering (ZITI)
Universität Heidelberg
B6, 23-29, Bauteil C
68131 Mannheim
GERMANY

 +49 (0) 621 181 2700
 +49 (0) 621 181 2695
 <https://oe.ziti.uni-heidelberg.de/joomla/de/berichte.html>

Layout: K.-H. Brenner, S. Volk

Type of publication: Online

Publication date: 2018

For quotation of any of these contributions, please use:

Reference: Annual Report 2017
Chair of Optoelectronics,
Universität Heidelberg
ISSN 2197 - 4462